Total cross sections and thermonuclear reaction rates for $^{13}C(d,n)$ and $^{14}C(d,n)$

C. R. Brune and R. W. Kavanagh
W. K. Kellogg Radiation Laboratory, California Institute of Technology, Pasadena, California 91125
(Received 12 November 1991)

The $^{13}C(d,n)$ and $^{14}C(d,n)$ cross sections have been measured for $0.2 \le E_{c.m.} \le 2.1$ MeV and $0.2 \le E_{c.m.} \le 1.3$ MeV, respectively, using a 4π neutron detector. The cross sections are used to calculate the thermonuclear reaction rates for temperatures below 10 GK. The implications of these and other new nuclear-physics results for inhomogeneous primordial nucleosynthesis are discussed.

PACS number(s): 25.45.Hi, 27.20.+n, 98.80.Ft

I. INTRODUCTION

The suggestion that the quark-hadron phase transition in the early Universe gave rise to a spatially inhomogeneous baryon density [1] has received much attention in recent years. The low-density regions will be relatively neutron rich, while the high-density regions will be relatively neutron poor because of the fact that neutrons, having no Coulomb interaction, diffuse much more readily than protons [2]. Subsequently, the nucleosynthesis taking place in these regions will differ from the standard model of big-bang nucleosynthesis [3], which assumes a homogeneous baryon density. The spatial scale and density profiles of the inhomogeneity are largely unknown because of uncertainties in the physics of the quark-hadron transition [4]. Recent calculations indicate that the initial hope of reconciling the observed light-element abundances with an $\Omega_b = 1$ universe is not fulfilled for reasonable constraints on the initial conditions [4]. However, the primordial production of heavy elements ($A > 7$) may provide a signature of inhomogeneity in the early Universe [5–8]. Heavy-element production is facilitated in the neutron-rich region, in which reactions involving neutron-rich isotopes are more effective in producing heavy elements. Kawano *et al.* [8] find significant CNO elemental production for a large region of parameter space in their two-zone model. Thus the observation of a "cosmic floor" for CNO abundances in metal-poor stars could be evidence of inhomogeneous nucleosynthesis.

The following sequence has been proposed [9] as the primary path to $A > 12$:

$$^{3}H(\alpha,\gamma)^{7}Li(n,\gamma)^{8}Li(\alpha,n)^{11}B(n,\gamma)^{12}B(\beta^{-}\nu)^{12}C(n,\gamma)^{13}C(n,\gamma)^{14}C\ .$$

Further reactions that consume ^{14}C have received close attention in two recent studies [8,10]. It was noted in Ref. [8] that many deuteron-induced reactions have been neglected in the reaction networks used to calculate heavy-element abundances. These reactions are typically strong, with high Q values, and the deuteron mass fraction during nucleosynthesis in the neutron-rich regions is estimated to be $\gtrsim 10^{-3}$. In particular, it was suggested that the reaction $^{14}C(d,n)$ may dominate ^{14}C consumption in the big bang.

In their study [8], Kawano *et al.* calculated the $^{14}C(d,n)$ rate using an S factor (see Sec. III) of 3.6×10^{6} keV b, estimated using a statistical nuclear model. In the energy range relevant to the big bang, the $^{14}C(d,n)$ reaction ($Q_0 = 7.983$ MeV) proceeds to several final states of ^{15}N, all of which are particle bound. The reaction has been studied by Chiba [11], who measured the ground-state neutron group at 0° for $E_d > 1$ MeV and made a slow-neutron survey for $E_d > 0.4$ MeV. Subsequently, Imhof, Grench, and Johnson [12] measured the cross section and angular distribution of the ground-state group for $E_d > 1$ MeV. The relevant quantity for nuclear astrophysics is the cross section to all final states, at low energies ($E_d \lesssim 1$ MeV). We report here measurements of the $^{14}C(d,n)$ cross section for $0.2 \le E_{c.m.} \le 1.3$ MeV, using a 4π neutron detector with a roughly constant neutron-detection efficiency. In addition, we have measured the total cross section for $^{13}C(d,n)$ in the energy range $0.2 \le E_{c.m.} \le 2.1$ MeV. The $^{13}C(d,n)$ reaction ($Q_0 = 5.326$ MeV) is similar to $^{14}C(d,n)$ in many respects (Q value, available final states, Coulomb barrier) and may also be important in inhomogeneous nucleosynthesis. Previous low-energy studies of the $^{13}C(d,n)$ reaction include that of Richardson [13], who measured the relative neutron yield at forward angles for $E_d > 0.2$ MeV; Marion, Bonner, and Cook [14], who found a slow-neutron threshold at $E_d = 0.44$ MeV; and James [15], who measured the angular distribution and relative strengths of the various neutron groups for $E_d > 1$ MeV.

II. EXPERIMENTAL METHOD

The 3-MV Pelletron Tandem Accelerator at the Kellogg Radiation Laboratory was used to provide the proton, deuteron, $^{3}He^{+}$, and $^{4}He^{+}$ beams used in this experiment. Beam energy was determined by a 90° magnetic analyzer and NMR gaussmeter calibrated ($\pm0.1\%$) using the 483.91 ± 0.10-keV resonance [16] in $^{19}F(p,\alpha\gamma)$, the

 ©1992 The American Physical Society

991.86±0.03-keV resonance [17] in ^{27}Al(p,γ), and the 606.0±0.5-keV resonance [18] in ^{11}B(α,n). Beam line and target vacuum were maintained $<7\times10^{-7}$ Torr.

A. Neutron detection

The neutron yields were measured using a 4π detector described in more detail elsewhere [19,20]. The detector consists of thermal-neutron detectors (11 ^{3}He-filled proportional counters) embedded in a polyethylene-cube moderator, with the bombarded target at the center. The efficiency of the detector was calibrated to be 20.2%, using a weak ^{252}Cf source ($\bar{E}_n=2.3$ MeV) with strength known to 3%. Previous tests using the ^{7}Li(p,n) reaction indicate that the efficiency is constant within 5% from 50 keV to 2 MeV. However, the neutrons in this experiment range up to an energy of about 8 MeV, where some decrease in efficiency is expected.

In order to estimate the neutron-detection efficiency for the ^{13}C(d,n) and ^{14}C(d,n) reactions, we employed the ^{9}Be(^{3}He,n)^{11}C reaction ($Q_0=7.557$ MeV), which also has numerous accessible final states and a similar Q value. The number of ^{11}C nuclides produced (and hence neutrons) was determined by measuring the delayed β^+ particles resulting from ^{11}C decay ($t_{1/2}=1223.1\pm1.2$ s) [21]. Thus, by comparing the number of neutrons detected with the number inferred from the delayed ^{11}C activity, the absolute efficiency can be deduced. The measurement was performed using a 70-μg/cm^2 ^{9}Be target and a 1.30-MeV ^{3}He beam. A 0.4-cm-diam collimator 1.8 cm from the target defined the beam spot and confined the positrons to a small volume of space. A -400-V suppression ring between the target and collimator and $+300$ V on the target ensured accurate beam-current integration. Positrons were detected via their 511-keV annihilation radiation by placing a 7.6-cm-diam, 7.6-cm-long NaI(Tl) scintillator at 0°, ~12 cm from the target. The photopeak efficiency was calibrated by placing in the target position an ^{26}Al source whose strength was calibrated previously using a high-purity-germanium γ-ray detector and calibration sources of known strength.

The neutron yield (in counts/μC) from the target was determined using a weak (~20 nA) beam, in order to minimize dead time in the neutron detector. The delayed activity was then produced using a steady 300-nA bombardment of known charge and duration, after which the scintillator was promptly placed in the counting position and positron measurements were begun. Prior to the delayed-activity production, scintillator measurements were made to establish the amount of ^{11}C present ($\lesssim5\%$ of that produced) from beam tuning and previous runs. The delayed-activity counting subsequent to production was continued for about 4000 s, recorded every 300 s. No evidence for decay half-lives other than that of ^{11}C was found. However, the ^{9}Be(^{3}He,αn)^{7}Be reaction ($Q=14$ keV), which produces neutrons but not ^{11}C, is energetically possible. In order to test for this possibility, the target (where all ^{7}Be produced is presumed to reside) was monitored for the 0.478-MeV γ rays resulting from ^{7}Be decay, using the germanium detector. A 0.478-MeV peak was found, and using the known ^{7}Be half-life (53.29±0.07 days) [22] and branching ratio (10.45±0.04%) [23] to ^{7}Li(0.478 MeV), the ratio ^{9}Be(^{3}He,αn)^{7}Be/^{9}Be(^{3}He,$n_{\rm tot}$) is found to be 13±3%. Using this correction, the neutron efficiency is found to be 18±2%, which is assumed to hold for neutrons from the ^{14}C(d,n) reaction.

The study of the ^{13}C(d,n) reaction at $E_d=1.2$ MeV by James [15] found that ~70% of the neutron yield results from transitions leaving the residual ^{14}N in its 4.91- and 5.69-MeV excited states. Thus the majority of the neutrons produced have energies below 2 MeV. We assume a similar energy distribution at lower bombarding energies and take the neutron efficiency for ^{13}C(d,n) to be 20.2±1.0%. The efficiency for neutrons from the reactions ^{13}C(α,n) and ^{14}C(p,n), used for target-thickness calibrations described below, was taken to be 20.2±0.6% because of the lower ($\lesssim3$ MeV) neutron energies involved.

A complication of using a deuteron beam on a solid target is the fact that a deuterium concentration builds up in the target as bombardment proceeds, giving rise to a background of neutrons from ^{2}H(d,n). The effect is typically most important at low energies, where the yield of the reaction under study is very low, while the yield of ^{2}H(d,n) is still high. An upper limit on the magnitude of the effect is easily estimated by assuming that all implanted deuterium lies at the surface of the target, assuming uniform beam intensity within a circle of one-half of the collimator diameter and using the well known, monotonically increasing ^{2}H(d,n) cross section [24]. The effect was studied experimentally by bombarding a platinum blank with a 200-keV deuteron beam and observing the neutron yield increase with accumulated beam charge. The observed yield was 20% of the calculated upper limit. During the ^{13}C(d,n) and ^{14}C(d,n) runs, a careful record was kept of all deuterium implanted in the targets, in order to estimate the effect of accumulated deuterium. In addition, all beam-defining collimators near the neutron detector, which could also give rise to this background, were replaced during each target change. Although this effect ultimately limited our low-energy sensitivity, we are confident that background arising from ^{2}H(d,n) contributes an error of $\lesssim5\%$ to the cross sections reported in this paper.

B. ^{13}C(d,n)

The relationship between cross section and number of neutrons detected, N_n, is given by

$$N_n=(nt)\sigma\epsilon N_i\ , \tag{1}$$

where N_i is the number of incident particles (determined by beam-current integration), (nt) is the areal number density of target atoms, σ is the cross section under study, and ϵ is the neutron-detection efficiency. The ^{13}C(d,n) cross section was measured with three different targets. The neutron yield was measured for $0.26\le E_d\le1.0$ MeV using a ~5-μg/cm^2 ^{13}C target produced by cracking ^{13}C-enriched iodo-methane on a tungsten substrate. In order to measure the yield at lower energy, a thicker (~40 μg/cm^2) target, produced in

the same manner, was employed. The principal advantage of using a thicker target is decreased sensitivity to background from ^{2}H(d,n). Measurements were performed at $E_d=0.213$, 0.561, and 1.000 MeV, with excellent agreement (for the last two energies) in energy dependence with the previous data. Further measurements were made using a 13-μg/cm^2 ^{13}C foil described in more detail below. The neutron yield was measured for $E_d=0.561$ MeV and for $1.0 \leq E_d \leq 2.4$ MeV, also in excellent agreement in energy dependence in the region of overlap with previously mentioned data.

The absolute normalization of the data was determined using a self-supported, 99%-enriched, ^{13}C foil on a stainless-steel frame with 8-mm aperture. The ^{13}C areal density was determined using both Rutherford scattering and alpha-particle energy loss. The Rutherford-scattering measurements were performed by bombarding the foil with ^{4}He$^+$ at 0.800 and 1.000 MeV (where the cross section is assumed to be governed by the Rutherford law), taking energy loss in the target into account in determining the energy at which to evaluate the cross section. The scattered alpha particles were detected at $\theta_{\rm lab}=165°$ with a silicon surface-barrier detector collimated to have a solid angle of 1.18 ± 0.02 msr. The result of the measurements was an areal density of $(6.04\pm0.22)\times10^{17}$ ^{13}C/cm^2.

In addition, elastic alpha-scattering measurements were made at $E_\alpha=2.000$ MeV in order to assess the contaminants present in the foil. The resulting detector spectrum is shown in Fig. 1. The primary contaminant observed was ^{12}C, with a number density about 5% of ^{13}C. The two-peak energy distribution of alpha particles scattered from ^{12}C was consistent with ^{12}C being on the front and back surfaces of the foil (this observation is also consistent with the manufacturer's claim of >99% ^{13}C enrichment). The next most prominent contaminant was oxygen, present at 2% by number, distributed uniformly throughout the foil. The remaining heavier contaminants totaled ~0.5% by number. The continuum in Fig. 1 up to channel 500 is presumed to be due to multiple scattering from collimator edges and other hardware.

The ^{13}C areal density was also determined using the observed widths of the narrow resonances in ^{13}C(α,n) at $E_\alpha=1.054$ and 1.59 MeV ($\Gamma_{\rm lab}=1.8$ keV and $\Gamma_{\rm lab}<0.13$ keV, respectively) [25]. The observed neutron yield as a function of bombarding energy in the vicinity of the 1.054-MeV resonance is shown in Fig. 2. The observed widths (22.0 ± 0.2 and 18.5 ± 0.2 keV at $E_\alpha=1.054$ and 1.59 MeV, respectively), after a 2% correction for oxygen contamination, are equal to the ^{13}C areal density times the stopping power for alpha particles in carbon. Using an uncertainty of 3% for the stopping power [26], we find $(5.96\pm0.20)\times10^{17}$ ^{13}C/cm^2 for the areal density. This result is in excellent agreement with that found using elastic scattering; the weighted average $(6.00\pm0.15)\times10^{17}$ ^{13}C/cm^2 is adopted for all further computations. In addition, the total cross section for ^{13}C(α,n) is determined to be 146 ± 7 μb at $E_\alpha=1.000$ MeV, and the thick-target yield of the 1.054-MeV resonance is 4410 ± 170 neutrons per μC (for pure ^{13}C).

C. ^{14}C(d,n)

The ^{14}C(d,n) cross section was measured using a 20-μg/cm^2 ^{14}C target (>95% enriched) on a platinum backing. The ^{14}C areal density was determined to be $(7.97\pm0.60)\times10^{17}$ nuclides/cm^2, using the neutron yield from ^{14}C(p,n) at $E_p=1310$ keV, where the (p,n) cross section has a broad peak with 290±20-mb cross section [18]. It should be mentioned that data [27] from the ^{14}N(n,p)^{14}C reaction, converted to ^{14}C(p,n) using detailed balance, yield an approximately 20% higher value for the peak cross section. The (d,n) yield was measured for $0.2<E_d<1.5$ MeV, in 20-keV steps for $E_d<1.0$ MeV. Lower-energy measurements were attempted, but significant and uncertain ^{2}H(d,n) contamination rendered the data unusable.

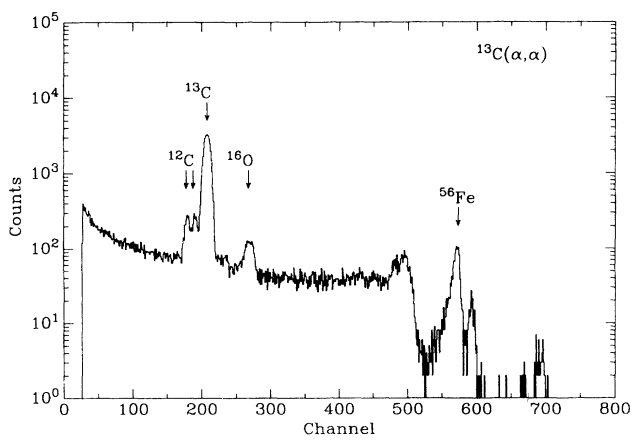

FIG. 1. Spectrum of scattered 2.000-MeV alpha particles at $\theta_{\rm lab}=165°$ from the self-supported ^{13}C foil. Primary contaminants are observed to be ^{12}C (on the surfaces of the foil) and ^{16}O.

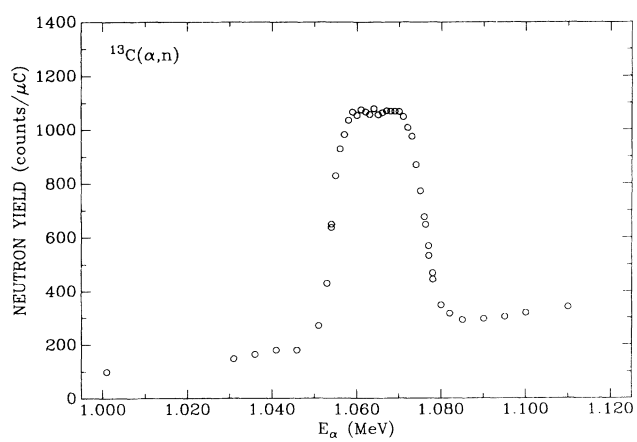

FIG. 2. Observed ^{13}C(α,n) excitation function in the vicinity of the 1.054-MeV resonance. The observed width, 22.0 ± 0.2 keV, is due to alpha-particle energy loss in the target and is used, together with the data of Fig. 1, to determine the ^{13}C areal density as described in the text.

III. RESULTS

A. $^{13}C(d,n)$

The astrophysical S factor, $S(E)$, is defined by

$$\sigma(E)=\frac{S(E)}{E}\exp(-\sqrt{E_G/E}\,)\,, \tag{2}$$

where E is the center-of-mass energy and E_G is the Gamow energy (61.453 MeV for $^{13}C+d$). For the lowest energies involved in this experiment, the cross section is strongly energy dependent, as characterized by the exponential barrier factor in Eq. (2). Since the beam loses energy as it passes through the target, one must determine the average or effective beam energy to associate with the cross section in Eq. (1). The properly weighted energy (ignoring straggling effects) is defined by the equation

$$\sigma(\bar{E}_d)=\frac{\int_{E_d-\Delta E}^{E_d}\sigma(E')\left[\frac{dE}{dx}(E')\right]^{-1}dE'}{\int_{E_d-\Delta E}^{E_d}\left[\frac{dE}{dx}(E')\right]^{-1}dE'}\,, \tag{3}$$

where $\bar{E}_d$ is the effective energy, E_d is the bombarding energy, $dE(E')/dX$ is the stopping power [26], and ΔE is the energy loss in the target. The equation was solved by assuming that the energy dependence of the cross section is given by Eq. (2), with constant S. The ^{13}C areal densities of the two targets on solid backings were determined by requiring that they coincide in cross-section scale with data obtained using the foil target. The scale uncertainty in the resulting cross sections is estimated to be 10%. The data are presented in Fig. 3, and the results for $S(E)$ [Eq. (2)] are plotted in Fig. 4.

It is seen from the plot of the S factor that there is no structure clearly identifiable as a "resonance," although there are peaks at 0.52 and 0.80 MeV. Perhaps there is evidence for the $^{13}C(d,n)^{14}N(5.69\ \text{MeV})$ threshold at $E_{c.m.}=0.37$ MeV seen previously by Marion, Bonner, and Cook [14]. Resonances in (d,n) have been reported at $E_{c.m.}=0.50$, 0.74, 1.34, and 1.54 MeV by Richardson [13]. A resonance in (d,p) at $E_{c.m.}=0.54$ MeV was reported by Koudijs, Valckx, and Endt [28] and confirmed by Marion and Weber [29], who also found complicated structure at higher energies. A summary of all known resonances in $^{13}C+d$ given by Marion and Weber [30] includes resonances at $E_{c.m.}=0.55$, 0.74, 0.95, 1.07, 1.21, 1.34, 1.42, 1.54, 1.56, 1.90, and 1.93 MeV. James [15] found that the angular distributions of some of the final states contributing to $^{13}C(d,n)$ were characteristic of the stripping mechanism, while the angular distributions of other final states were characteristic of compound-nucleus formation. In view of the lack of definitive structure observed for the S factor, no attempt was made to fit the data with resonance parameters.

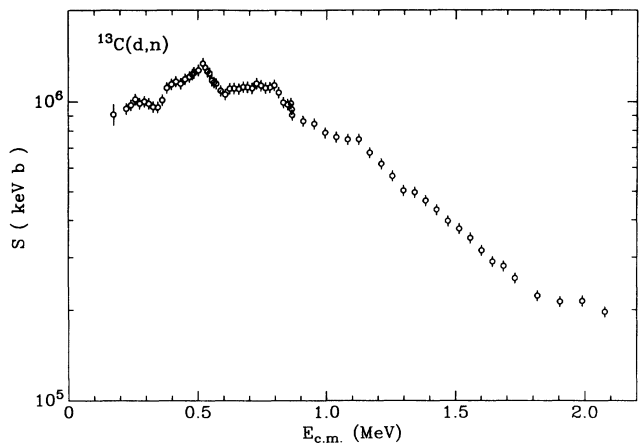

FIG. 4. S factor for $^{13}C(d,n)$, calculated from the data of Fig. 3.

B. $^{14}C(d,n)$

The data for $^{14}C(d,n)$ were analyzed in the same manner as for the $^{13}C(d,n)$ data, the only change being in E_G, which is 62.051 MeV for $^{14}C+d$. The cross section, with scale uncertainty estimated to be 15%, is plotted in Fig. 5, and the S factor is presented in Fig. 6. In contrast

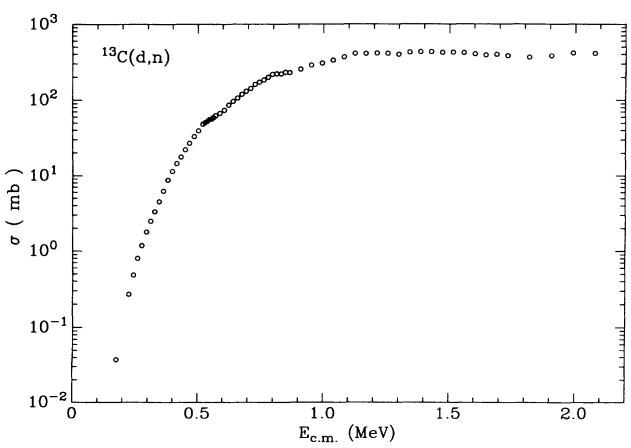

FIG. 3. Total cross section for $^{13}C(d,n)$ found in this experiment. Relative errors are smaller than the size of the plot points; the normalization uncertainty is estimated to be 10%.

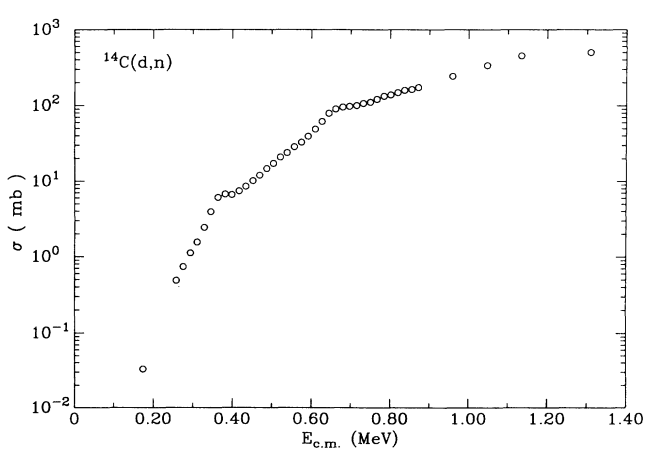

FIG. 5. Total cross section for $^{14}C(d,n)$. The relative errors are smaller than the size of the data points. The normalization uncertainty of the data is estimated to be 15%.

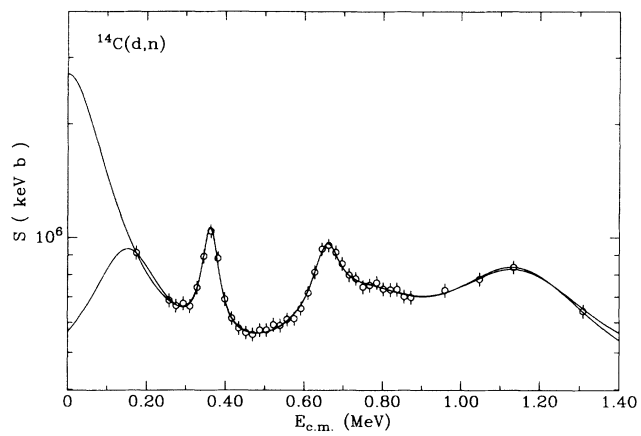

FIG. 6. S factor for $^{14}C(d,n)$, calculated from the data of Fig. 5. The solid curves are fits to Eq. (4) for different assumptions concerning the low-energy behavior (see Table I).

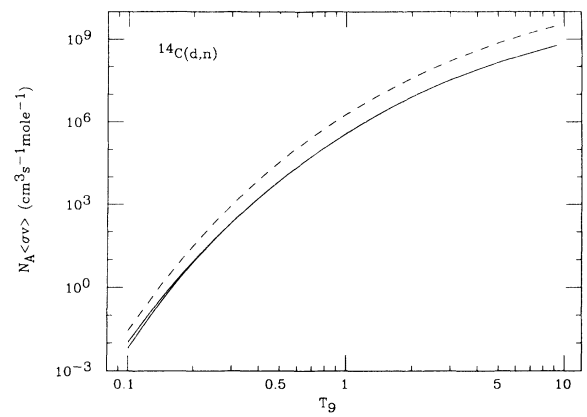

FIG. 8. Thermonuclear reaction rate $N_A\langle\sigma v\rangle$ for $^{14}C(d,n)$. The solid curves were calculated assuming that the S factor is given by the fitted curves in Fig. 5, extrapolated as discussed in the text. Equation (7) is an analytic approximation (±4%) to the average of the two curves. The dashed curve is the rate used in Ref. [8].

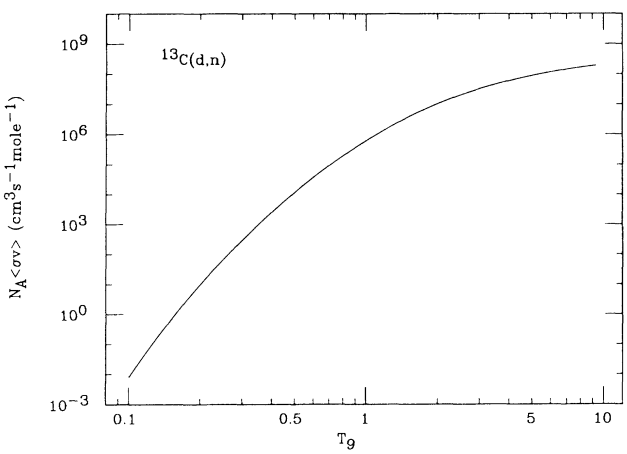

FIG. 7. Thermonuclear reaction rate $N_A\langle\sigma v\rangle$ for $^{13}C(d,n)$ calculated from our data and extrapolation as described in the text. Equation (6) is an analytic approximation (±4%) for this rate.

to the $^{13}C(d,n)$ reaction, the S factor for $^{14}C(d,n)$ shows some definite resonance structure; hence the S factor was fitted with the form

$$S(E)=H_0+\sum_{i=1}^{5}\frac{H_i(\Gamma_i/2)^2}{(E-E_i)^2+(\Gamma_i/2)^2}\ . \tag{4}$$

Because of the unknown behavior of the cross section below the range of our data, fits using two different assumptions for that behavior were performed, as shown in Fig. 6 (the fit parameters are listed in Table I). All of the parameters of Eq. (4) were varied, with the exception of the energy of the lowest resonance (E_1), which was fixed at $E_{c.m.}=0.000$ and 0.150 MeV for the fits in Table I labeled 1 and 2, respectively. The energies and widths of the other resonance terms were not significantly changed between the two fits, and so they were forced to be identical. We assume that the true low-energy S factor below the range of our data lies between the two curves shown. Resonances are clearly observed at $E_{c.m.}=0.362\pm0.004$

TABLE I. Parameters returned by fits of Eq. (4) to $S(E)$ for $^{14}C(d,n)$ for two different assumptions concerning low-energy extrapolation as discussed in text.

	i	H_i (keV b)	E_i (MeV)	Γ_i (MeV)
Fit 1	0	$(3.33\pm0.33)\times10^5$		
	1	$(2.35\pm0.70)\times10^6$	0.0	0.187±0.029
	2	$(5.05\pm0.37)\times10^5$	0.362±0.004	0.047±0.004
	3	$(3.25\pm0.39)\times10^5$	0.657±0.005	0.078±0.006
	4	$(2.42\pm0.19)\times10^5$	0.753±0.027	0.340±0.068
	5	$(4.45\pm0.27)\times10^5$	1.141±0.018	0.423±0.070
Fit 2	0	$(3.86\pm0.31)\times10^5$		
	1	$(5.07\pm1.00)\times10^5$	0.150	0.199±0.042
	2	$(5.22\pm0.37)\times10^5$	0.362±0.004	0.047±0.004
	3	$(3.23\pm0.39)\times10^5$	0.657±0.005	0.078±0.006
	4	$(2.22\pm0.21)\times10^5$	0.753±0.027	0.340±0.068
	5	$(3.96\pm0.29)\times10^5$	1.141±0.018	0.423±0.070

and 0.657±0.005 MeV with widths $\Gamma_{c.m.}=47\pm4$ and 78±6 keV, corresponding to excitation energies in ^{16}N of $E_x=10.836\pm0.004$ and 11.131±0.005 MeV, respectively. The three other resonance terms required to fit the data are not clearly related to resonances in the compound nucleus.

The fact that the ^{14}C(d,n) reaction can proceed by the compound-nucleus mechanism was demonstrated by Chiba [11], who found a resonance for the ground-state group at $E_{c.m.}=1.14$ MeV with width $\Gamma_{c.m.}=190$ keV, as well as others at higher energy. Imhof, Grench, and Johnson [12] verified the resonance findings of Chiba and found the total cross section of the ground-state neutron group to be roughly 75 mb for $1.0<E_{c.m.}<2.0$ MeV. Our results for the cross section to all ^{15}N final states is 3–7 times larger in the region of overlap, indicating that the cross section to the excited states is dominant. Neither of the two resonances definitely found in our experiment was seen in the study by Zeitnitz *et al.* [31], who measured the total neutron cross section of ^{15}N over the excitation energy range in the ^{16}N nucleus corresponding to our experiment. However, a state with $E_x=11.16\pm0.04$ MeV was found in the ^{13}C$(\alpha,p)^{16}$N experiment of Hamill, Peterson, and Yasue [32], which corresponds in energy with the state at $E_x=11.131\pm0.005$ MeV found here.

C. Reaction rates

The thermonuclear reaction rate $N_A\langle\sigma v\rangle$ for nonidentical particles is given by [33]

$$N_A\langle\sigma v\rangle=\left[\frac{8}{\mu\pi}\right]^{1/2}\frac{N_A}{(kT)^{3/2}}\int_0^\infty\sigma(E)E\exp\left[-\frac{E}{kT}\right]dE\ , \tag{5}$$

where μ is the reduced mass in the entrance channel, k is Boltzmann's constant, T is the temperature, and E is the energy in the center of mass. For ^{13}C(d,n) the integration was performed numerically, using linear interpolation of the S factor between data points for the range of energies measured in the experiment, a constant S factor of 9.0×10^5 keV b for energies below the range measured, and a constant cross section of 410 mb for energies greater than the range measured. The resulting reaction rate as a function of T_9, the temperature in GK, is plotted in Fig. 7; the reaction rate is given (within 4% of the rate calculated by the above procedure for $T_9\le10$) by the analytic expression

$$N_A\langle\sigma v\rangle=3.54\times10^{12}T_9^{-2/3}\exp\left[-\frac{16.885}{T_9^{1/3}}\right]\left[1-0.134T_9^{2/3}+\frac{4.35}{T_9^{4/3}-1.92T_9^{2/3}+2.43}\right]. \tag{6}$$

Energies between 0.2 and 2.1 MeV (i.e., the range covered by this experiment) make up at least 50% of the integrand in Eq. (5) for $0.2\le T_9\le10$.

The reaction rate for ^{14}C(d,n) was calculated in a manner similar to that for ^{13}C(d,n). The rate was calculated for each fit to Eq. (4), using the fit to extrapolate to zero energy; for energies above the range covered experimentally, a constant S factor of 6.42×10^5 keV b was assumed. The reaction rates resulting from the two fits are shown (as solid lines) in Fig. 8. For astrophysical purposes it seems most reasonable to take the average of the two calculated rates, which is given (within 4% of the calculated rate for $T_9\le10$) by the expression

$$N_A\langle\sigma v\rangle=8.07\times10^{12}T_9^{-2/3}\exp\left[-\frac{16.939}{T_9^{1/3}}\right]\left[1+\frac{0.046}{T_9^{4/3}+0.032}+\frac{0.040}{T_9^{4/3}-3.62T_9^{2/3}+3.69}\right]. \tag{7}$$

Energies in the range covered by the experiment contribute at least 50% of the rate calculated for $0.2\le T_9\le3$. The rate for this reaction assumed previously [8] is also plotted (as a dashed line) in Fig. 8 and is seen to be about a factor of 7 larger than that found here experimentally.

IV. DISCUSSION AND CONCLUSION

The ^{13}C(d,n) reaction rate has been calculated using the cross sections measured in this experiment. It is possible that ^{13}C(d,n) may play an important role in inhomogeneous big-bang nucleosynthesis, especially in light of the recent measurement [34] of the competing ^{13}C(n,γ) cross section, which resulted in an order-of-magnitude smaller reaction rate than previously used. New nucleosynthesis calculations, making use of the latest reaction rates, are needed to identify the important reactions on ^{13}C.

In Ref. [8] it was shown that the dominant depletion reactions on ^{14}C in the inhomogeneous big bangs are ^{14}C(p,γ), ^{14}C(n,γ), and ^{14}C(d,n) (depending somewhat on the region of parameter space investigated). The reaction rate for ^{14}C(d,n) found in this experiment is roughly a factor of 7 smaller than the rate used in Ref. [8], decreasing the importance of this reaction. However, the ^{14}C(n,γ) cross section has been recently measured [35] at energies corresponding to $kT=25$ keV, yielding a result that is 5 times smaller than that estimated by Wiescher, Görres, and Thielemann [10] (and used in Ref. [8]) and a factor of 100 smaller than that used by Kajino, Mathews, and Fuller [7]. The ^{14}C(p,γ) cross section, measured by Görres *et al.* [36] in the energy range pertinent to primordial nucleosynthesis, was adopted by Ref. [8]. Clearly, there has been much progress in understanding the

nuclear reactions on ^{14}C, but the full implications of these results for inhomogeneous nucleosynthesis are not clear at this time.

Several other experimental results, pertaining to the chain of reactions (Sec. I) leading to production of heavy elements, warrant comment. The $^{7}Li(n,\gamma)$ reaction has been recently remeasured [37] at $E_n = 30$ keV; the result agrees with older work [38] and with a $1/v$ extrapolation of the thermal cross section [39], but is a factor of 2 higher than another recent measurement [40]. Measurements of the $^{8}Li(\alpha,n)^{11}B$ cross section [41] using a radioactive ^{8}Li beam (which determined the cross section to all final ^{11}B states) indicate that the cross section is approximately 5 times larger than that found in an experiment utilizing the inverse reaction [42] (which determined the cross section only to the ground state). In addition, the $^{12}C(n,\gamma)$ cross section has been measured [37] at $E_n = 30$ keV, reducing the uncertainty in this important reaction rate.

Considerable uncertainty still exists in the theoretical modeling of inhomogeneous primordial nucleosynthesis [43]. In particular, Terasawa and Sato [44] find that previous calculations significantly overestimated the heavy-element production, as a result of the use of an oversimplified model of neutron diffusion. On the observational side, perhaps the most promising possibilities are the observations, recently shown to be feasible [45], of ^{9}Be and ^{11}B in metal-poor stars.

ACKNOWLEDGMENTS

This work was supported in part by the National Science Foundation, Grant No. PHY88-17296.

[1] E. Witten, Phys. Rev. D **30**, 272 (1984).
[2] J. H. Applegate and C. J. Hogan, Phys. Rev. D **31**, 3037 (1985).
[3] T. P. Walker, G. Steigman, D. N. Schramm, K. A. Olive, and H. Kang, Astrophys. J. **376**, 51 (1991).
[4] H. Kurki-Suonio and R. A. Matzner, Phys. Rev. D **42**, 1047 (1990).
[5] R. A. Malaney and W. A. Fowler, Astrophys. J. Lett. **345**, L5 (1989).
[6] T. Kajino and R. N. Boyd, Astrophys, J. **359**, 267 (1990).
[7] T. Kajino, G. J. Mathews, and G. M. Fuller, Astrophys. J. **364**, 7 (1990).
[8] L. H. Kawano, W. A. Fowler, R. W. Kavanagh, and R. A. Malaney, Astrophys. J. **372**, 1 (1991).
[9] R. A. Malaney and W. A. Fowler, in *Origin and Distribution of the Elements*, edited by G. J. Mathews (World Scientific, Singapore, 1988), p. 76.
[10] M. Wiescher, J. Görres, and F. K. Thielemann, Astrophys. J. **363**, 340 (1990).
[11] R. Chiba, Phys. Rev. **123**, 1316 (1961).
[12] W. L. Imhof, H. A. Grench, and R. G. Johnson, Nucl. Phys. **49**, 503 (1963).
[13] J. E. Richardson, Phys. Rev. **80**, 850 (1950).
[14] J. B. Marion, T. W. Bonner, and C. F. Cook, Phys. Rev. **100**, 847 (1955).
[15] A. N. James, Nucl. Phys. **24**, 132 (1961).
[16] F. Ajzenberg-Selove, Nucl. Phys. **A475**, 1 (1987).
[17] P. M. Endt, Nucl. Phys. **A521**, 1 (1990).
[18] T. R. Wang, R. B. Vogelaar, and R. W. Kavanagh, Phys. Rev. C **43**, 883 (1991).
[19] S. E. Kellogg and R. W. Kavanagh, Bull. Am. Phys. Soc. **34**, 1192 (1989); (unpublished).
[20] C. R. Brune, R. W. Kavanagh, S. E. Kellogg, and T. R. Wang, Phys. Rev. C **43**, 875 (1991).
[21] F. Ajzenberg-Selove, Nucl. Phys. **A506**, 1 (1990).
[22] F. Ajzenberg-Selove, Nucl. Phys. **A490**, 1 (1988).
[23] R. T. Skelton and R. W. Kavanagh, Nucl. Phys. **A414**, 141 (1984).
[24] H. Liskien and A. Paulsen, Nucl. Data Tables **11**, 569 (1973).
[25] F. Ajzenberg-Selove, Nucl. Phys. **A460**, 1 (1986).
[26] J. F. Ziegler, *The Stopping and Ranges of Ions in Matter* (Pergamon, New York, 1977), Vols. 3 and 4.
[27] G. L. Morgan, Oak Ridge National Laboratory Report No. ORNL/TM-6528/R1, 1978; Nucl. Sci. Eng. **70**, 163 (1979).
[28] B. Koudijs, F. P. G. Valckx, and P. M. Endt, Physica **19**, 1133 (1953).
[29] J. B. Marion and G. Weber, Phys. Rev. **103**, 167 (1956).
[30] J. B. Marion and G. Weber, Phys. Rev. **102**, 1355 (1956).
[31] B. Zeitnitz, H. Dubenkropp, R. Putzki, G. J. Kirouac, S. Cierjacks, J. Nebe, and C. B. Dover, Nucl. Phys. **A166**, 443 (1971).
[32] J. J. Hamill, R. J. Peterson, and M. Yasue, Nucl. Phys. **A408**, 21 (1983).
[33] W. A. Fowler, G. R. Caughlan, and B. A. Zimmerman, Annu. Rev. Astron. Astrophys. **5**, 525 (1967).
[34] S. Raman, M. Igashira, Y. Dozono, H. Kitazawa, M. Mizumoto, and J. E. Lynn, Phys. Rev. C **41**, 458 (1990).
[35] H. Beer, M. Wiescher, F. Käppeler, J. Görres, and P. E. Koehler, Astrophys. J. (to be published).
[36] J. Görres, S. Graff, M. Wiescher, C. A. Barnes, H. W. Becker, and T. R. Wang, Nucl. Phys. **A517**, 329 (1990).
[37] Y. Nagai, K. Takeda, S. Motoyama, T. Ohsaki, M. Igashira, N. Mukai, F. Uesawa, T. Ando, H. Kitazawa, and T. Fukuda, Nucl. Instrum. Methods B **56/57**, 492 (1991).
[38] W. L. Imhof, R. G. Johnson, F. J. Vaughn, and M. Walt, Phys. Rev. **114**, 1037 (1959).
[39] J. E. Lynn, E. T. Jurney, and S. Raman, Phys. Rev. C **44**, 764 (1991).
[40] M. Wiescher, R. Steininger, and F. Käppeler, Astrophys. J. **344**, 464 (1989).
[41] R. N. Boyd, presented at Caltech Centennial Year Nuclear Astrophysics Symposium, 12–14 August 1991 (unpublished).
[42] T. Paradellis, S. Kossionides, G. Doukellis, P. Assimakopoulos, A. Pakou, C. Rolfs, and K. Langanke, Z. Phys. A **337**, 211 (1990).
[43] T. Kajino, Nucl. Instrum. Methods B **56/57**, 564 (1991).
[44] N. Terasawa and K. Sato, Astrophys. J. Lett. **362**, L47 (1990).
[45] G. Gilmore, B. Edvardsson, and P. E. Nissen, Astrophys. J. **378**, 17 (1991).